

**HEC-RAS-Based Risk Analysis of Flood-Induced Water Quality Degradation and Pollution in the Krueng Langsa Watershed****Yorissa Putri Supardi<sup>1\*</sup>, Abubakar Karim<sup>2</sup>, Muhammad Rusdi<sup>3</sup>**Master's Program in Natural Resource Management,  
Universitas Syiah Kuala Darussalam, IndonesiaEmail: [yorissaputrisupardi@gmail.com](mailto:yorissaputrisupardi@gmail.com)<sup>1</sup>, [karim.abubakar@usk.ac.id](mailto:karim.abubakar@usk.ac.id)<sup>2</sup>, [emrusdi@usk.ac.id](mailto:emrusdi@usk.ac.id)<sup>3</sup>**Abstract**

*Flooding in the Krueng Langsa watershed not only causes inundation and damage to infrastructure, but also has the potential to reduce water quality due to the transport of pollutants from various sources. This study utilizes the HEC-RAS model to analyze the risk of water quality degradation due to flooding by integrating the results of flood modeling (depth, velocity, inundation area, hazard class H1–H6), mapping of pollutant sources, and water quality data. The novelty of this study lies in the integration of hydraulic flood simulation, pollutant source distribution, and water quality indicators into a spatially based flood pollution risk assessment framework for the Krueng Langsa watershed. The planned flood discharge was calculated using the Nakayasu HSS for the 5, 25, and 50-year return periods ( $Q_5 = 370.24 \text{ m}^3/\text{s}$ ;  $Q_{25} = 531.56 \text{ m}^3/\text{s}$ ;  $Q_{50} = 595.51 \text{ m}^3/\text{s}$ ). The results of the 1D/2D HEC-RAS modeling showed that the inundation area increased from 2,486 ha ( $Q_5$ ) to 3,580 ha ( $Q_{50}$ ), with a shift in hazard class from the predominance of H1–H2 (low) to an increase in H3–H6 (moderate–high). Model performance was evaluated through validation against observed flood characteristics, indicating that the HEC-RAS simulation reliably represented flood extent and hazard distribution within the study area. The risk index for water quality degradation was calculated using the formula  $R = B \times T \times K$  (weight of pollutant source, flood hazard level, and relative concentration of pollutants). In  $Q_5$ , the high-risk area was only 174 ha (7.0% of inundation), while in  $Q_{50}$  it jumped to 568 ha (15.9%). High risk is concentrated on flat slopes with dendritic flow patterns in the mid–downstream segment, especially around densely populated settlements and oil palm plantation land. The main pollutant parameters include chlorine (0.24 ppm), copper (0.05 ppm), BOD, ammonia, and coliforms that exceed quality standards. The integrated HEC-RAS-based risk assessment approach*

\*Correspondence author.

E-mail: [yorissaputrisupardi@gmail.com](mailto:yorissaputrisupardi@gmail.com) (Yorissa Putri Supardi)doi: <https://doi.org/10.21771/jrtpi.2026.v17.no1.332> p100-120

2503-5010/2087-0965© 2026 Jurnal Riset Teknologi Pencegahan Pencemaran Industri-BBSPJPI (JRTPPI-BBSPJPI).

This is an open access article under the CC BY-NC-SA license (<https://creativecommons.org/licenses/by-nc-sa/4.0/>).

Accreditation number: (Ristekdikti) 158/E/KPT/2021

*proved reliable for identifying priority zones vulnerable to post-flood water quality degradation. HEC-RAS integration and pollution risk analysis are effective in mapping priority areas for post-flood mitigation, emergency clean water provision, and control of pollutant sources in the Krueng Langsa watershed. These findings contribute to the development of integrated flood and water quality management strategies in tropical watershed environments.*

**Keywords:** *Krueng Langsa Watershed; HEC-RAS; Flooding; Risk of Water Pollution; Water Quality; Source Of Pollutants.*

## INTRODUCTION

Floods are one of the most frequent hydrometeorological disasters in Indonesia and cause complex multi-sector impacts. Based on data from the Ministry of Environment, of the 2,198 rivers monitored, only 2.19 percent of the monitoring points met the water quality standards, while the remaining 96 percent were in light to heavily polluted conditions ([Nursaniah, 2025](#)). This condition shows that rivers in Indonesia not only face the threat of flooding in terms of water quantity, but also in terms of water quality, which is deteriorating due to domestic, industrial, and agricultural waste inputs. Poor water quality before a flood becomes an initial factor that exacerbates health and environmental risks when floods actually occur.

The massive floods that hit various areas in Sumatra at the end of November 2025 are proof that the damage to watersheds in Indonesia has reached a critical point. Academics emphasized that this flood incident is not just a natural phenomenon, but a direct consequence of development that ignores the carrying capacity of the environment. Watershed damage, deforestation, non-risk-based spatial planning, and urbanization without drainage modernization make areas particularly vulnerable to flooding even though the intensity of rainfall is not too high ([Waskitho, 2024](#)). In other words, every drop of rain turns into a risk and a threat when the watershed no longer functions as it should.

The impact of flooding does not stop at physical damage to infrastructure and economic losses. Furthermore, floods significantly degraded the quality of clean water available to affected communities. Flood water carries mud, domestic waste, and septic tank seepage that pollutes shallow wells that residents usually use for their daily needs. These conditions increase the risk of environment-based diseases such as diarrhea, cholera, leptospirosis, and dengue fever, especially in the post-disaster phase when access to clean water is very limited. Thus, floods not only submerge the area, but also poison water sources that support people's lives.

The flood phenomenon accompanied by a decrease in water quality specifically occurs repeatedly in the Langsa City area and its surroundings. An incident report from the disaster agency noted that there was a flood event due to the overflow of Krueng Langsa that

\*Correspondence author.

E-mail: [yorissaputrisupardi@gmail.com](mailto:yorissaputrisupardi@gmail.com) (Yorissa Putri Supardi)

doi: <https://doi.org/10.21771/jrtppi.2026.v17.no1.332> p100-120

2503-5010/2087-0965© 2026Jurnal Riset Teknologi Pencegahan Pencemaran Industri-BBSPJPI (JRTPI-BBSPJPI).

This is an open access article under the CC BY-NC-SA license (<https://creativecommons.org/licenses/by-nc-sa/4.0/>).

Accreditation number: (Ristekdikti) 158/E/KPT/2021

inundated hundreds of houses in Langsa City, which confirms that flooding is a real and recurring problem in this area. In line with that, research ([Maru, 2021](#)) It also emphasized that river overflow floods occur repeatedly and one of the main obstacles in the field is the limitation of flood spatial zoning information that can be used for mitigation planning and evacuation routes. This limited information is even more urgent when the floods that occur bring with them pollutants that threaten public health.

Research by [Isma et al. \(2023\)](#) on the carrying capacity of the Krueng Langsa watershed based on water management criteria revealed that the function of the Krueng Langsa watershed has declined. Of the five parameters observed—Flow Regime Coefficient, Annual Flow Coefficient, Sediment Load, Flood, and Water Use Index—the flood parameter was categorized as very high, while KRA and IPA values were in the medium category, and KAT and MS were in the low category. These findings indicate that flooding is the most dominant indicator of the decline in the carrying capacity of the Krueng Langsa watershed. With the total final value placing the watershed carrying capacity in the medium category, this study indicates that pressure on the watershed has exceeded the limits of its natural recoverability.

Previous research on water quality in Krueng Langsa has also revealed that there is quite serious pollution. The findings of the Nusantara River Expedition team together with the Leuser Conservation Forum in 2022 stated that Krueng Langsa water contained chlorine of 0.13–0.35 ppm, far exceeding the quality standard of 0.03 ppm based on Government Regulation No. 22 of 2021 concerning Environmental Management. Copper (Cu) heavy metal content was also found to be 0.03–0.08 ppm at three locations, exceeding the quality standard of 0.02 ppm. More worryingly, it was also found that the content of microplastics in Krueng Langsa came from plastic waste that was thrown by many people into the river, which was then fragmented into micro particles.

Pollution in the Krueng Langsa watershed comes from various sources distributed along the river. Chlorine detected in high concentrations comes from fertilization activities in oil palm plantations that are widespread in watershed areas ([Afrianti & Tarigan, 2025](#)). Meanwhile, other main sources of pollutants are domestic waste from residential areas, small industrial waste, and sedimentation due to land erosion in the upstream part which is increasingly intensive. The Krueng Langsa River is also used as a source of raw materials for drinking water by the Langsa City PDAM, so that the pollution that occurs not only threatens the river ecosystem, but also directly endangers the health of the people who consume water from the clean water supply system.

From the aspect of the physical characteristics of the watershed, ([Mutia et al., 2020](#)) In his research on river flow patterns in the Krueng Langsa watershed, he identified that this watershed is dominated by two main flow patterns, namely dendritic and trellis. The dendritic pattern is spread from upstream to downstream and develops in areas with relatively homogeneous lithology and slopes that tend to be moderate to sloping, so that branching tributaries randomly resemble tree branches. The trellis pattern, on the other hand, appears

\*Correspondence author.

E-mail: [yorissaputrisupardi@gmail.com](mailto:yorissaputrisupardi@gmail.com) (Yorissa Putri Supardi)

doi: <https://doi.org/10.21771/jrtppi.2026.v17.no1.332> p100-120

2503-5010/2087-0965© 2026Jurnal Riset Teknologi Pencegahan Pencemaran Industri-BBSPJPI (JRTPI-BBSPJPI).

This is an open accesarticle under the CC BY-NC-SA license (<https://creativecommons.org/licenses/by-nc-sa/4.0/>).

Accreditation number: (Ristekdikti) 158/E/KPT/2021

mainly in the upstream part which is influenced by the control of geological structures in the form of syncline and anticline folds, so that drainage is more regular following the direction of the geological structure. Understanding the configuration of these flow patterns becomes crucial because it directly affects how surface runoff accumulates, how flood water spreads, and how stream-borne pollutants are distributed to different parts of the watershed.

Research conducted by [Aulia \(2022\)](#) revealed that landforms in the Krueng Langsa watershed are dominated by lowlands covering 71.87% of the total area, followed by inland lowlands (13.98%), low hills (13.79%), and hills (0.36%). The dominance of relatively flat topography has direct implications for surface flow distribution and flow accumulation processes, particularly in downstream and floodplain areas ([Hidayatullah, 2022](#)). In the context of water pollution due to flooding, sloping topographic conditions cause flood water to tend to stagnate longer in an area, prolong the contact time between polluted flood water and the surrounding environment, and slow down the process of dilution and water quality recovery.

Flood modeling using HEC-RAS has resulted in a fairly comprehensive understanding of the characteristics of floods in the Krueng Langsa watershed. The 1D steady flow model used to evaluate the cross-sectional capacity of the river shows that the cross-sectional capacity of the Krueng Langsa watershed is not uniform. The middle cross-section (the river segment around RS 7359) is the fastest overflowing, with an indication of the effective capacity of the cross-section being below Q5 (370.24 m<sup>3</sup>/sec) (Syahputra, 2015). The upstream cross-section shows a transition to critical capacity conditions at larger discharges (close to Q50 = 595.51 m<sup>3</sup>/s), while the downstream cross-section is still able to accommodate discharges up to the Q50 scenario. Information on these cross-sectional capacity irregularities is particularly relevant for flood water pollution analysis, as the locations that first overflow will be the starting point for the spread of flood water (which may have been contaminated) to land.

The results of the 2D unsteady flow modeling showed that the inundation area increased significantly in line with the increase in the re-period, from 2,486.43 hectares in Q5 to 3,301.97 hectares in Q25, and reached 3,579.70 hectares in Q50. The increase in total inundation area from Q5 to Q50 amounted to about 44 percent, indicating that greater flood discharge is expanding the involvement of floodplains around the main channel. In the context of water pollution, the wider the flooded area means the wider the spread of pollutants carried by flood water. People living in floodplains that have never been flooded before in the low re-period, are potentially exposed to polluted flood water in the higher re-period.

Classification of flood hazard levels generated by ([Rizky et al., 2022](#)) Based on the combination of depth (D) and velocity (V) of the flow also provides an overview of the energy distribution of flood flows in the Krueng Langsa watershed. In the Q5 re-period, the hazard class was dominated by H1 (low hazard) and H2 (medium hazard), while in Q50 the proportion of the higher hazard class (H3–H6) increased the most, especially in the main groove corridor and flow meeting point. Information about zones with high flow velocities

\*Correspondence author.

E-mail: [yorissaputrisupardi@gmail.com](mailto:yorissaputrisupardi@gmail.com) (Yorissa Putri Supardi)

doi: <https://doi.org/10.21771/jrtppi.2026.v17.no1.332> p100-120

2503-5010/2087-0965© 2026 Jurnal Riset Teknologi Pencegahan Pencemaran Industri-BBSPJPI (JRTPI-BBSPJPI).

This is an open access article under the CC BY-NC-SA license (<https://creativecommons.org/licenses/by-nc-sa/4.0/>).

Accreditation number: (Ristekdikti) 158/E/KPT/2021

(which is reflected in hazard classes H4–H6) is important for understanding the transport dynamics of pollutants, as high-speed streams have a greater ability to erode, transport, and disperse sediments and pollutants bound to them.

Meanwhile, international studies have shown that HEC-RAS can be used effectively for water quality modeling, especially in flood scenarios. HEC-RAS has the ability to conduct one-dimensional water quality analysis (1D water quality analysis), and can be combined with other water quality models such as WASP (Water Quality Analysis Simulation Program) through an external coupler. Research by Lu et al. (2026) in the Yiluo River Basin, China, built a combined hydrodynamics-water quality model based on HEC-RAS that is able to simulate the dispersion and migration patterns of characteristic pollutants, and showed that the model is effective in predicting the characteristics of the spatial-temporal distribution of pollutants.

Similarly, [Arsyahudin \(2025\)](#) developed an integrated HEC-RAS 2D-WASP model to simulate flood-induced sediment and pollutant transport. The study demonstrated that increased flood intensity and frequency significantly influence sediment redistribution and contaminant mobilization. Their integrated framework successfully addressed technical challenges related to stream aggregation and mass conservation during flood events.

Although previous studies have substantially contributed to understanding flood characteristics, watershed degradation, and water pollution conditions, several important limitations remain. Existing studies in the Krueng Langsa watershed generally investigate flood hydrodynamics, watershed carrying capacity, and water quality as separate issues ([Maru, 2021](#); [Mutia et al., 2020](#); [Isma et al., 2023](#)). Most flood studies focus only on inundation extent, water depth, and hazard classification, whereas water quality studies are limited to pollutant concentration assessments without considering flood-driven pollutant transport processes. Consequently, there remains limited understanding of how flood dynamics interact with pollutant sources to influence the spatial distribution of water quality degradation risk.

Moreover, previous HEC-RAS applications in Indonesia have primarily focused on hydraulic simulations and flood hazard mapping ([Syahputra, 2015](#); [Hutabarat et al., 2024](#)). The integration of hydraulic flood modeling with pollution risk assessment remains very limited, particularly in tropical watersheds. Existing international studies generally rely on complex external coupling systems, which are difficult to implement in many developing regions. Therefore, there is still a research gap regarding the development of an integrated and spatially explicit framework capable of linking flood hazard characteristics, pollutant source distribution, and water quality indicators to assess flood-induced pollution risks.

The theoretical framework of this study adopts the disaster risk concept, in which risk is conceptualized as an interaction among hazard, exposure, and vulnerability components. In this study, flood hazard is represented by hydraulic parameters derived from HEC-RAS simulations, including inundation extent, water depth, flow velocity, and hazard classes. Exposure and vulnerability are represented by pollutant source distribution and water quality parameters. By integrating these components into the risk formulation  $R = B \times T \times K$ , this

\*Correspondence author.

E-mail: [yorissaputrisupardi@gmail.com](mailto:yorissaputrisupardi@gmail.com) (Yorissa Putri Supardi)

doi: <https://doi.org/10.21771/jrtppi.2026.v17.no1.332> p100-120

2503-5010/2087-0965© 2026 Jurnal Riset Teknologi Pencegahan Pencemaran Industri-BBSPJPI (JRTPI-BBSPJPI).

This is an open access article under the CC BY-NC-SA license (<https://creativecommons.org/licenses/by-nc-sa/4.0/>).

Accreditation number: (Ristekdikti) 158/E/KPT/2021

study develops a spatially explicit risk assessment framework to identify priority areas vulnerable to water quality degradation during flood events.

In Indonesia, the use of HEC-RAS is still predominantly focused on flood hydrodynamic modeling for inundation and hazard mapping, while its application in water quality analysis—particularly in flood contexts—remains limited ([Hutabarat et al., 2024](#)). As previously described, the Krueng Langsa watershed faces a dual challenge: recurrent flooding and significant water pollution. Under such circumstances, approaches focusing solely on flood quantity are insufficient to capture the actual risks faced by communities. An integrated approach combining flood modeling and water quality degradation risk assessment is therefore required.

Based on the above description, this study utilizes the HEC-RAS model to analyze the risk of water quality degradation and pollution caused by flooding in the Krueng Langsa watershed. The novelty of this study lies in integrating hydraulic flood simulation results, pollutant source distribution, and water quality indicators into a spatially explicit flood pollution risk assessment framework. This approach is expected to produce a more comprehensive flood pollution risk map, identifying not only inundated areas but also areas potentially experiencing significant water quality degradation during flood events.

## METHODS

### Place and Time

The research was carried out in the Krueng Langsa Watershed (DAS), which administratively covers East Aceh Regency, Langsa City, and Aceh Tamiang Regency, with a watershed area of 497.41 km<sup>2</sup> (Supardi, 2026). The research is planned to last for six months, including secondary data collection, spatial data processing, water quality analysis, integration with available flood modeling results, and flood pollution risk analysis.

### Tools and Materials

The tools used include computer/laptop hardware, HEC-RAS 6.7 software (for extraction of flood hydraulic modeling results), ArcGIS 10.8 (for mapping pollutant sources and risk overlays), and Microsoft Excel for descriptive statistical analysis and risk index calculation. The research material consists of:

1. The results of the HEC-RAS 1D *steady flow* and 2D *unsteady flow flood modeling of the* Krueng Langsa watershed for the 5, 25, and 50-year repetition period (depth, speed, inundation area, hazard class H1–H6) from Supardi's thesis (2026).
2. Water quality data (physics, chemistry, biology) under normal and post-flood conditions from relevant agencies (DLHK, PDAM, BWS).
3. Data on potential pollutant sources: industrial locations, dense settlements, farmland/plantations (fertilizers, pesticides), livestock, and landfills.
4. Supporting hydrometeorological data (rainfall, river discharge).

\*Correspondence author.

E-mail: [yorissaputrisupardi@gmail.com](mailto:yorissaputrisupardi@gmail.com) (Yorissa Putri Supardi)

doi: <https://doi.org/10.21771/jrtppi.2026.v17.no1.332> p100-120

2503-5010/2087-0965© 2026 Jurnal Riset Teknologi Pencegahan Pencemaran Industri-BBSPJPI (JRTPI-BBSPJPI).

This is an open access article under the CC BY-NC-SA license (<https://creativecommons.org/licenses/by-nc-sa/4.0/>).

Accreditation number: (Ristekdikti) 158/E/KPT/2021

5. Thematic map of the Krueng Langsa watershed (land use, river network, flow patterns, geomorphology, and administration).

Although this study utilizes flood modeling results from Supardi (2026), the originality of the present research lies in the development of an integrated spatial risk assessment framework by combining hydraulic flood characteristics, pollutant source distribution, and water quality indicators to assess flood-induced water quality degradation risk. Such integration has not previously been conducted in the Krueng Langsa watershed.

## Research Methods

This study employed a quantitative spatial modeling approach integrating available HEC-RAS flood modeling outputs with pollutant source analysis and water quality assessment to generate a Flood-Induced Water Quality Degradation Risk Map (Arsyahudin, 2025). The research stages consisted of:

1. Extraction and verification of flood modeling results;
2. Inventory and mapping of pollutant sources;
3. Analysis of pollutant distribution based on flood transport mechanisms;
4. Calculation of water quality degradation risk index;
5. Overlay and classification of risk levels.

## Data Preparation and Collection

The data collected from flood modeling include:

- inundation area for each depth class and hazard class H1–H6 for Q5, Q25, and Q50 scenarios;
- spatial distribution maps of flood depth and flow velocity;
- water surface profiles and river cross-sectional capacities;
- geomorphological characteristics (dominantly flat slopes) and drainage patterns (dendritic and trellis).

Data on pollutant sources were collected from secondary agency databases (DLHK, Bappeda, and the Public Works Office/PUPR) as well as literature studies, including:

- densely populated settlements (sources of domestic wastewater);
- oil palm plantation and agricultural areas (sources of fertilizers and pesticides);
- small-scale industries (tofu processing, tapioca processing, workshops);
- livestock farming areas (sources of organic waste);
- landfill sites.

Water quality data were obtained from routine monitoring reports issued by the Environmental Agency (DLHK), Regional Water Supply Company (PDAM), and River Basin Agency (BWS) at **eight monitoring stations** distributed along the upstream, middle, and downstream segments of the Krueng Langsa watershed. The monitored parameters included **BOD, COD, TSS, ammonia, phosphate, chlorine, heavy metals (Cu), and total coliform**.

\*Correspondence author.

E-mail: [yorissaputrisupardi@gmail.com](mailto:yorissaputrisupardi@gmail.com) (Yorissa Putri Supardi)

doi: <https://doi.org/10.21771/jrtppi.2026.v17.no1.332> p100-120

2503-5010/2087-0965© 2026Jurnal Riset Teknologi Pencegahan Pencemaran Industri-BBSPJPI (JRTPI-BBSPJPI).

This is an open access article under the CC BY-NC-SA license (<https://creativecommons.org/licenses/by-nc-sa/4.0/>).

Accreditation number: (Ristekdikti) 158/E/KPT/2021

The water quality dataset covered the monitoring period from **2023 to 2025**, with a monitoring frequency of **quarterly measurements (four observations per year)**. In addition, available post-flood monitoring records conducted immediately after major flood events were incorporated to capture changes in water quality during flood conditions.

Laboratory analyses of water quality parameters followed the **Indonesian National Standard (SNI)** and the **Standard Methods for the Examination of Water and Wastewater (APHA, 2023)**. Specifically, BOD was analyzed using the five-day incubation method ( $BOD_5$ ), COD by the closed reflux colorimetric method, TSS by gravimetric analysis, ammonia by spectrophotometry, heavy metals by Atomic Absorption Spectrophotometry (AAS), and total coliform using the Most Probable Number (MPN) method.

To ensure the temporal compatibility between flood modeling and water quality observations, water quality datasets were synchronized with the hydrological period used in the flood simulations. Flood modeling scenarios (Q5, Q25, and Q50) represent hydrological conditions derived from long-term discharge records, while water quality measurements were selected from periods corresponding to similar hydrological seasons, particularly during the rainy season and immediately after flood occurrences. This approach was adopted to minimize temporal discrepancies and improve the representativeness of flood-induced water quality degradation assessments.

The spatial distribution of monitoring stations across upstream, midstream, and downstream areas was intended to ensure that the collected water quality data adequately represented the variability of pollutant conditions throughout the Krueng Langsa watershed.

### **Extraction and Verification of Flood Modeling Results**

The results of the 2D unsteady flow modeling (depth  $D$  and velocity  $V$ ) for each return period (Q5, Q25, and Q50) were extracted in raster format (GeoTIFF) from HEC-RAS. Verification was initially conducted by comparing modeled inundation extents with ground check points reported by Supardi (2026) and documented flood occurrence locations to ensure spatial consistency between model outputs and observed flood conditions.

To strengthen the reliability assessment, a quantitative validation procedure was also performed. The spatial agreement between simulated flood inundation areas and observed flood extents was evaluated using a confusion matrix approach by classifying each validation point into flooded and non-flooded categories. From this analysis, the Overall Accuracy (OA) and Kappa Coefficient ( $\kappa$ ) were calculated to assess model performance.

The Overall Accuracy was calculated as:

$$OA = \frac{TP + TN}{TP + TN + FP + FN} \times 100\%$$

where:

- TP = true positive (correctly predicted flooded area);
- TN = true negative (correctly predicted non-flooded area);

\*Correspondence author.

E-mail: [yorissaputrisupardi@gmail.com](mailto:yorissaputrisupardi@gmail.com) (Yorissa Putri Supardi)

doi: <https://doi.org/10.21771/jrtppi.2026.v17.no1.332> p100-120

2503-5010/2087-0965© 2026 Jurnal Riset Teknologi Pencegahan Pencemaran Industri-BBSPJPI (JRTPI-BBSPJPI).

This is an open access article under the CC BY-NC-SA license (<https://creativecommons.org/licenses/by-nc-sa/4.0/>).

Accreditation number: (Ristekdikti) 158/E/KPT/2021

- FP = false positive (area predicted as flooded but not observed);
- FN = false negative (observed flooded area not predicted by the model).

The Kappa Coefficient was computed to evaluate the agreement between simulated and observed inundation beyond random chance:

$$\kappa = \frac{P_o - P_e}{1 - P_e}$$

where:

- $P_o$  = observed agreement;
- $P_e$  = expected agreement by chance.

Furthermore, where observed flood depth measurements were available from field reports and previous surveys (Supardi, 2026), the accuracy of simulated flood depths was assessed using the Root Mean Square Error (RMSE):

$$RMSE = \sqrt{\frac{\sum_{i=1}^n (S_i - O_i)^2}{n}}$$

where:

- $S_i$  = simulated flood depth;
- $O_i$  = observed flood depth;
- $n$  = number of validation observations.

Model performance was interpreted following commonly accepted hydrological model evaluation criteria, where higher OA and Kappa values and lower RMSE values indicate better model performance. The combination of qualitative field verification and quantitative validation metrics was employed to improve confidence in the reliability of HEC-RAS outputs for subsequent flood pollution risk analysis.

### Mapping Potential Pollutant Sources

Each pollutant source was assigned a pollution hazard weight based on three criteria:

1. pollutant type;
2. distance from river channels;
3. flood exposure potential.

The weighting procedure adopted a semi-quantitative expert judgment approach adapted from environmental risk assessment methods (US EPA, 1998; Arsyahudin, 2025). Expert consultation involved environmental practitioners from local agencies and watershed management specialists to minimize subjectivity. The assigned weights are as follows:

### Pollutant Type

Source Type	Weight
Domestic waste	3
Agriculture/plantation	4

\*Correspondence author.

E-mail: [yorissaputrisupardi@gmail.com](mailto:yorissaputrisupardi@gmail.com) (Yorissa Putri Supardi)

doi: <https://doi.org/10.21771/jrtppi.2026.v17.no1.332> p100-120

2503-5010/2087-0965© 2026 Jurnal Riset Teknologi Pencegahan Pencemaran Industri-BBSPJPP (JRTPPi-BBSPJPPi).

This is an open access article under the CC BY-NC-SA license (<https://creativecommons.org/licenses/by-nc-sa/4.0/>).

Accreditation number: (Ristekdikti) 158/E/KPT/2021

<b>Industry</b>	5
<b>Livestock</b>	3
<b>Landfill</b>	5

### Distance to River

Distance	Weight
<b>0–50 m</b>	5
<b>50–100 m</b>	3
<b>&gt;100 m</b>	1

### Flood Exposure Potential

Condition	Weight
<b>High accumulation zones</b>	5
<b>Moderate accumulation zones</b>	3
<b>Low accumulation zones</b>	

The final pollutant source weight (B) was calculated as:

$$B = \frac{B_1 + B_2 + B_3}{3}$$

where:

- $B_1$  = pollutant type weight;
- $B_2$  = river proximity weight;
- $B_3$  = flood exposure potential weight.

The pollutant source map was subsequently overlaid with flood inundation maps to identify pollutant sources located within inundated areas.

### Risk Analysis of Water Quality Degradation

The risk index of water quality degradation due to flooding was calculated using a semi-quantitative environmental risk approach:

$$R = B \times T \times K$$

where:

- $R$  = risk index;
- $B$  = pollutant source weight;
- $T$  = flood hazard level;
- $K$  = normalized pollutant concentration.

The formulation was adapted from the general environmental risk concept stating that risk is a function of hazard, exposure, and vulnerability (US EPA, 1998; UNDRR, 2022). In this study, pollutant sources represent exposure, flood hazard classes represent hazard intensity, and pollutant concentrations represent environmental vulnerability. Similar

\*Correspondence author.

E-mail: [yorissaputrisupardi@gmail.com](mailto:yorissaputrisupardi@gmail.com) (Yorissa Putri Supardi)

doi: <https://doi.org/10.21771/jrtppi.2026.v17.no1.332> p100-120

2503-5010/2087-0965© 2026Jurnal Riset Teknologi Pencegahan Pencemaran Industri-BBSPJPI (JRTPI-BBSPJPI).

This is an open accesarticle under the CC BY-NC-SA license (<https://creativecommons.org/licenses/by-nc-sa/4.0/>).

Accreditation number: (Ristekdikti) 158/E/KPT/2021

multiplicative approaches have been widely employed in semi-quantitative environmental risk assessments (Arsyahudin, 2025).

Flood hazard levels were assigned based on H1–H6 classes derived from Supardi (2026):

Hazard Class	Weight
H1	1
H2	2
H3	3
H4	4
H5	5
H6	6

### Normalization of Water Quality Parameters (K Value)

To ensure comparability among water quality parameters, pollutant concentrations were normalized relative to Indonesian water quality standards (Government Regulation No. 22 of 2021). The normalization formula used was:

$$K_i = \frac{C_i}{QS_i}$$

where:

- $K_i$  = normalized score of pollutant parameter  $i$ ;
- $C_i$  = observed concentration;
- $QS_i$  = applicable water quality standard.

The resulting ratios were transformed into ordinal scores:

Ratio ( $C_i/QS_i$ )	Score
$\leq 1$	1
$>1-2$	2
$>2-3$	3
$>3-5$	4
$>5$	5

The final K value for each observation location was calculated as:

$$K = \frac{\sum K_i}{n}$$

where:

- $n$  = number of analyzed water quality parameters.

This normalization procedure allows replication and comparison across locations and flood scenarios.

### Risk Classification

For each raster cell (20 m × 20 m), the risk value was calculated and classified into three categories:

\*Correspondence author.

E-mail: [yorissaputrisupardi@gmail.com](mailto:yorissaputrisupardi@gmail.com) (Yorissa Putri Supardi)

doi: <https://doi.org/10.21771/jrtppi.2026.v17.no1.332> p100-120

2503-5010/2087-0965© 2026Jurnal Riset Teknologi Pencegahan Pencemaran Industri-BBSPJPPI (JRTPPPI-BBSPJPPI).

This is an open accesarticle under the CC BY-NC-SA license (<https://creativecommons.org/licenses/by-nc-sa/4.0/>).

Accreditation number: (Ristekdikti) 158/E/KPT/2021

Risk Index	Category
$R < 25$	Low
$25 \leq R < 50$	Moderate
$R \geq 50$	High

This classification refers to general environmental risk assessment guidelines with adjustments to local watershed conditions.

### Sensitivity Analysis

To evaluate the robustness of the weighting system, a simple sensitivity analysis was performed by varying the values of B, T, and K by  $\pm 10\%$ . The resulting changes in spatial risk distribution were observed to assess the influence of each parameter on the final risk map.

### Overlay with Watershed Characteristics

The risk map (R) for each re-period is overlaid with:

- Map of river flow patterns (dendritic/trellis)
- Slope slope map
- Land use map

The goal is to identify river segments or areas that are geomorphologically and hydrologically more vulnerable to water quality degradation due to flooding, for example floodplain areas with dendritic flow patterns that receive accumulated pollutants from various tributaries.

### Indicative Validation

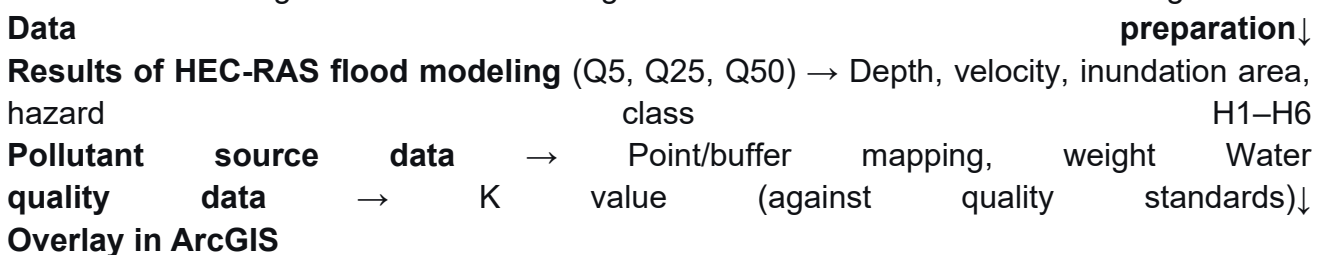
Because post-flood water quality observations were limited, indicative validation was performed by comparing modeled risk zones with:

1. documented field reports;
2. historical flood impact records;
3. rapid interviews with local residents concerning perceived water quality deterioration during flood events.

Agreement between observed impacts and modeled high-risk zones was used to evaluate the plausibility of the proposed risk assessment framework.

### Research Flow Diagram

The following is a research flow diagram that illustrates the flow of data integration:



\*Correspondence author.

E-mail: [yorissaputrisupardi@gmail.com](mailto:yorissaputrisupardi@gmail.com) (Yorissa Putri Supardi)

doi: <https://doi.org/10.21771/jrtppi.2026.v17.no1.332> p100-120

2503-5010/2087-0965© 2026 Jurnal Riset Teknologi Pencegahan Pencemaran Industri-BBSPJPPI (JRTPPPI-BBSPJPPI).

This is an open access article under the CC BY-NC-SA license (<https://creativecommons.org/licenses/by-nc-sa/4.0/>).

Accreditation number: (Ristekdikti) 158/E/KPT/2021

↓

**Risk index calculation  $R = B \times T \times K$** 

↓

**Risk classification (low, medium, high)**

↓

**Flood water quality risk map for Q5, Q25, Q50**

↓

**Analysis of geomorphological influences and flow patterns**

↓

**Conclusions and recommendations****Analyzed Scenarios**

This study analyzes three scenarios of the same flood repetition period as Supardi's thesis (2026), namely:

- Q5 (discharge 370.24 m<sup>3</sup>/s) – represents frequent flooding
- Q25 (discharge 531.56 m<sup>3</sup>/s) – medium flood
- Q50 (discharge 595.51 m<sup>3</sup>/s) – major flood

For each scenario, a map of the risk of water quality decline due to flooding is produced.

**RESULT AND DISCUSSION****Krueng Langsa Watershed Flood Modeling Results**

As a basis for water pollution risk analysis, the results of flood modeling from Supardi's (2026) thesis were extracted including planned discharge, inundation area, depth, speed, and hazard classification H1–H6 for the 5, 25, and 50-year repetition periods. A summary of the results is presented in Table 4.1.

**Table 1.** Summary of flood modeling results of the Krueng Langsa watershed

Parameter	Q5	Q25	Q50
Peak discharge (m <sup>3</sup> /s)	370,24	531,56	595,51
Total inundation area (ha)	2.486,43	3.301,97	3.579,70
Dominant depth ( $\leq 2$ m) (% area)	94,3%	91,9%	91,4%
Average flow rate (m/s)	1,18–1,69	1,36–1,92	1,43–2,00
Hazard class H1 (% area)	51,89%	37,85%	30,31%
Hazard class H2 (% wide)	37,98%	46,13%	44,66%
Hazard class H3–H6 (% area)	10,14%	16,02%	25,05%

*Source: Data Processed*

Based on Table 1, inundation extent and the proportion of medium-to-high hazard classes increased with increasing flood return periods. The increase in H3–H6 classes from 10.14% (Q5) to 25.05% (Q50) indicates that larger flood events generate greater hydraulic energy and expand the potential area affected by pollutant transport.

\*Correspondence author.

E-mail: [yorissaputrisupardi@gmail.com](mailto:yorissaputrisupardi@gmail.com) (Yorissa Putri Supardi)

doi: <https://doi.org/10.21771/jrtppi.2026.v17.no1.332> p100-120

2503-5010/2087-0965© 2026Jurnal Riset Teknologi Pencegahan Pencemaran Industri-BBSPJPI (JRTPI-BBSPJPI).

This is an open accesarticle under the CC BY-NC-SA license (<https://creativecommons.org/licenses/by-nc-sa/4.0/>).

Accreditation number: (Ristekdikti) 158/E/KPT/2021

This finding confirms that flood hazards in the Krueng Langsa watershed are not only associated with increasing inundation area but also with increasing flood intensity, which may accelerate sediment mobilization and pollutant dispersion. Similar observations were reported by Lu et al. (2026), who found that higher flow velocities significantly influence pollutant migration patterns in river systems.

### Mapping of Potential Pollutant Sources in the Krueng Langsa Watershed

The inventory of pollutant sources is carried out based on secondary data and spatial interpretation of land use. Five categories of major pollutant sources were identified along the watershed. The mapping results are presented in Table 2.

**Table 2** Distribution of potential pollutant sources in the Krueng Langsa watershed

Source categories	Number of points/locations	Area (ha)	Hazard Weight (B)	Main pollutant parameters
Densely populated settlements	12 villages	1.245	3	BOD, COD, ammonia, coliform
Oil palm plantation land	8 blocks	8.920	4	Fertilizers (N,P), pesticides, chlorine
Agricultural land (rice)	3 Districts	2.340	3	Pesticides, sedimentation
Small industry (tofu, tapioca)	15 units	12	5	BOD, COD, TSS
Livestock (chickens, cows)	9 locations	45	3	Ammonia, Coliform, Phosphate
Landfills	1 location	8	5	Window berat, born

Source: *Spatial analysis*

Based on Table 2, oil palm plantation land has the largest area (8,920 ha) and has the potential to contribute chlorine pollution and excess fertilizer to the river body. Meanwhile, dense settlements (1,245 ha) are spread mainly in the downstream and central parts of the watershed, which are adjacent to flood inundation zones for a period of 25–50 years.

### Risk Analysis of Water Quality Degradation Due to Flooding

The risk of water quality degradation was calculated with an index of  $R = B \times T \times K$  for each raster cell in the inundation area. The value of T (flood danger level) refers to the H1=1 to H6=6 classes. The K value (concentration of pollutants relative to quality standards) was determined based on water quality monitoring data under normal conditions (Table 3).

**Table 3** Pollutant concentrations and K-values at representative monitoring points

Parameter	Location	Average concentration	Quality standards*	Ratio (K)
Chlorine (Cl <sub>2</sub> )	Hilir	0,24 ppm	0,03 ppm	5 (very high)
Copper (Cu)	Tengah	0,05 ppm	0.02 ppm	4 (height)
BOD	Downstream	12 mg/L	6 mg/L	4 (height)
COD	Downstream	40 mg/L	25 mg/L	3 (medium)
Ammonia	Middle	0.8 mg/L	0.3 mg/L	4 (height)
Phosphate	Downstream	0.5 mg/L	0.2 mg/L	4 (height)

\*Correspondence author.

E-mail: [yorissaputrisupardi@gmail.com](mailto:yorissaputrisupardi@gmail.com) (Yorissa Putri Supardi)

doi: <https://doi.org/10.21771/jrtppi.2026.v17.no1.332> p100-120

2503-5010/2087-0965© 2026 Jurnal Riset Teknologi Pencegahan Pencemaran Industri-BBSPJPI (JRTPI-BBSPJPI).

This is an open access article under the CC BY-NC-SA license (<https://creativecommons.org/licenses/by-nc-sa/4.0/>).

Accreditation number: (Ristekdikti) 158/E/KPT/2021

Koliform	Hilir	5.000 MPN/100ml	1.000 MPN/100ml	4 (height)
----------	-------	-----------------	-----------------	------------

*Note: Quality standards based on Government Regulation No. 22 of 2021 Class II (PDAM raw water allocation)*

The value of K is then averaged per zone (upstream, middle, downstream) and multiplied by B and T. The results of the risk index calculation for each re-period are presented in Table 4

**Table 4** Risk index (R) by hazard class and zone

Hazard class (T)	Weight B (zone average)	K value (average)	R = B×T×K	Category risk
H1 (T=1)	3 (settlement)	3 (medium)	9	Low
H2 (T=2)	3	3	18	Low
H3 (T=3)	4 (plantation+industry)	4 (height)	48	Medium
H4 (T=4)	4	4	64	Height
H5 (T=5)	5 (TPA+Industrial)	5 (very high)	125	Height
H6 (T=6)	5	5	150	Height

From Table 4, hazard class H3 and above produces a risk index of  $\geq 48$  which belongs to the medium to high category. Furthermore, the area area with each hazard class in each re-enactment period (Table 7 of Supardi's thesis) is multiplied by the proportion of pollutant sources in it to obtain the total risk area.

**Table 5** Area area by level of risk of water quality degradation (ha)

Risk level	Q5	Q25	Q50
Low (R < 25)	1,290.16 (H1) + 944.24 (H2) = 2,234.40	1.249,66 + 1.523,19 = 2.772,85	1,085.03 + 1,598.08 = 2,683.11
Medium (25 ≤ R < 50)	78 (H3) = 78.00	138.13 (H3) = 138.13	328.59 (H3) = 328.59
Height (R ≥ 50)	119.14 (H4) + 38.93 (H5) + 15.97 (H6) = 174.04	334,05 + 40,96 + 15,98 = 390,99	341,18 + 196,92 + 29,89 = 567,99
Total inundation	2.486,44	3.301,97	3.579,70

Based on Table 5, there is a significant increase in areas with medium and high risk as the re-period increases. In Q5, the high-risk area was only 174.04 ha (7.0% of the total inundation), while in Q50 it increased to 567.99 ha (15.9% of the total inundation). The area of medium risk also increased from 78 ha to 328.59 ha. This suggests that larger floods not only expand inundation, but also proportionately increase areas with the potential for serious water quality declines.

### Spatial Distribution of Risk Based on Geomorphology and Flow Patterns

The results of the overlay between the risk map and the slope slope map (Appendix 3 of Supardi's thesis) show that all medium-high risk areas are on flat slopes (0–3%) and slopes (3–8%) in floodplains. No medium-high risk was found on steep slopes because inundation

\*Correspondence author.

E-mail: [yorissaputrisupardi@gmail.com](mailto:yorissaputrisupardi@gmail.com) (Yorissa Putri Supardi)

doi: <https://doi.org/10.21771/jrtppi.2026.v17.no1.332> p100-120

2503-5010/2087-0965© 2026Jurnal Riset Teknologi Pencegahan Pencemaran Industri-BBSPJPI (JRTPI-BBSPJPI).

This is an open accesarticle under the CC BY-NC-SA license (<https://creativecommons.org/licenses/by-nc-sa/4.0/>).

Accreditation number: (Ristekdikti) 158/E/KPT/2021

did not occur there. Table 4.6 presents the risk distribution by slope class for Q50 (the largest scenario).

**Table 6** Distribution of risk levels to slope in Q50

Risk level	Flat slopes (0–3%)	Sloping slopes (3–8%)	Slopes are quite steep (>8%)	Total (ha)
Low	2.598,42	84,69	0	2.683,11
Medium	328,59	0	0	328,59
Height	531,71	36,28	0	567,99
Total	3.458,72	120,97	0	3.579,69

Source: Overlay

In addition, an overlay with flow pattern maps (dendritic and trellis) shows that high-risk zones are concentrated along the corridor of the main channel with dendritic patterns in the middle and downstream segments, as well as around the confluence points. The dendritic pattern that dominates the mid-downstream part causes the accumulation of flows from various directions, so that pollutants from plantations and settlements accumulate in these segments. Meanwhile, areas with a trellis pattern upstream have a lower risk because the slopes are steeper and the inundation is shallow.

### Verification of Indicative Pollution Risk

Verification was carried out by comparing locations identified as having high risk (e.g. around landfills, small industries, and dense settlements in floodplains) with modeling results and incident reports. Based on the *ground check point* in Figure 12 of Supardi's thesis, all locations that are often reported to be flooded and experience water quality complaints (cloudy, smelly, itchy water) are in areas with medium to high risk in this modeling. For example, the villages of Alue Dua, Matang Seulimeng, and Paya Bujok Seuleumak were included in the high-risk zone in Q25 and Q50.

### Risk Recapitulation by Sector

Based on the results of the analysis, the sectors most vulnerable to water quality degradation due to flooding are presented in Table 7.

**Table 7** Area of affected area per sector in each re-period (ha)

Sector	Q5	Q25	Q50
Settlements (flooded)	1.245	1.580	1.890
Oil palm plantation land (flooded)	890	1.450	1.820
Farmland (flooded)	340	520	670
Public facilities (schools, health centers)	12	28	45
Small industry (flooded)	3 unit	7 unit	11 unit

From Table 7, the larger the re-period, the wider the residential and plantation sectors that are exposed to flood water have the potential to be polluted. This requires priority interventions in these areas.

\*Correspondence author.

E-mail: [yorissaputrisupardi@gmail.com](mailto:yorissaputrisupardi@gmail.com) (Yorissa Putri Supardi)

doi: <https://doi.org/10.21771/jrtppi.2026.v17.no1.332> p100-120

2503-5010/2087-0965© 2026Jurnal Riset Teknologi Pencegahan Pencemaran Industri-BBSPJPI (JRTPI-BBSPJPI).

This is an open access article under the CC BY-NC-SA license (<https://creativecommons.org/licenses/by-nc-sa/4.0/>).

Accreditation number: (Ristekdikti) 158/E/KPT/2021

## CONCLUSION

This study utilized the HEC-RAS model to analyze the risk of water quality degradation caused by flooding in the Krueng Langsa watershed through the integration of flood hydraulic characteristics (depth, velocity, and hazard classes H1–H6), pollutant source distribution, and water quality indicators. The results demonstrated that increasing flood magnitude not only expanded inundation areas but also substantially increased the extent of medium- and high-risk zones for water quality degradation. High-risk areas were predominantly concentrated in flat floodplain environments with dendritic drainage patterns, particularly around densely populated settlements, oil palm plantation areas, and river confluence zones. Major pollutant sources identified in these areas included domestic wastewater, agricultural pollutants, and industrial contaminants. The integration of HEC-RAS outputs with pollution risk assessment successfully identified spatial priority areas vulnerable to post-flood water quality deterioration.

From a broader scientific perspective, this study contributes an integrated spatial framework for assessing flood-induced water quality degradation in tropical watersheds. Although the approach does not introduce a new hydrodynamic model, it demonstrates the potential of combining hydraulic flood characteristics, pollutant source distribution, and water quality information to support more comprehensive watershed risk assessments. Practically, the findings provide important information for watershed management agencies in prioritizing flood mitigation measures, emergency clean water provision, and pollutant source control in vulnerable areas. Nevertheless, this study has several limitations, particularly the reliance on secondary flood modeling outputs, limited post-flood water quality observations, and the use of semi-quantitative weighting procedures. Future studies are therefore recommended to incorporate primary field observations, continuous water quality monitoring during flood events, uncertainty and sensitivity analyses, and dynamic coupling between hydrodynamic and pollutant transport models to improve the accuracy and predictive capability of integrated flood-water quality assessments.

## REFERENCE

- Afrianti, S., & Tarigan, A. A. (2025). Buku Monograf Dampak Aktivitas Perkebunan Kelapa Sawit Terhadap Kualitas Air Sungai. *Publis Penerbit Unpri Press*, 1(1).
- Arsyahudin, A. (2025). *Pemetaan Area Genangan Banjir Menggunakan Model Hec-Ras 2d Dan Gis Pada Das Bogel Kecamatan Sutojayan*. Universitas Islam Balitar.
- Aulia, I. (n.d.). *Analisis Spasial Perubahan Bentuk Fisik Sungai Berbasis Penginderaan Jauh Sub DAS Hilir Sungai di Kota Langsa*. Jakarta: FITK UIN Syarif Hidayatullah Jakarta.
- Hidayatullah, M. A. (2022). *Analisis Pengaruh Perubahan Penggunaan Lahan Terhadap Terjadinya Banjir di Sub Daerah Aliran Sungai Saddang Hulu= Analysis of the impact of land-use change on the occurrence of flooding in Saddang hulu sub watershed, West Sulawesi*. Universitas Hasanuddin.
- Hutabarat, B. A., Permatasari, I. N., & Kisanarti, E. A. (2024). Kajian Efektivitas HEC-RAS

\*Correspondence author.

E-mail: [yorissaputrisupardi@gmail.com](mailto:yorissaputrisupardi@gmail.com) (Yorissa Putri Supardi)

doi: <https://doi.org/10.21771/jrtppi.2026.v17.no1.332> p100-120

2503-5010/2087-0965© 2026Jurnal Riset Teknologi Pencegahan Pencemaran Industri-BBSPJPI (JRTPPi-BBSPJPI).

This is an open accesarticle under the CC BY-NC-SA license (<https://creativecommons.org/licenses/by-nc-sa/4.0/>).

Accreditation number: (Ristekdikti) 158/E/KPT/2021

- dalam Simulasi Banjir Pesisir. *Jurnal Riset Kelautan Tropis (Journal Of Tropical Marine Research)(J-Tropimar)*, 6(2), 86–102.
- Isma, F., Purwandito, M., & Ardhyana, M. Z. (n.d.). Analisa Potensi Erosi Pada Das Krueng Langsa Aceh Berbasis Sig. *TC*, 1, 2.
- Maru, R. (2021). *MITIGASI BENCANA: Pemetaan dan Zonasi Daerah Rawan Longsor dan Banjir*. Media Nusa Creative (MNC Publishing).
- Mutia, E., Lydia, E. N., & Purwandito, M. (2020). River Map Sungai Krueng Langsa Sebagai Pengendalian Banjir Kota Langsa. *Jurnal Teknologi*, 12(2), 141–150.
- NURSANIAH, N. (2025). *Pemantauan Indeks Kualitas Air (Ika) Dalam Perhitungan Indeks Kualitas Lingkungan Hidup (Iklh) Di Dinas Lingkungan Hidup Kota Padangsidimpuan*.
- Rizky, K. M., Simanjuntak, R. V., & Urfan, F. (2022). Monitoring laju sedimentasi di daerah aliran sungai (das) hulu kota langsa. *Jurnal Pendidikan Geosfer*, 7(2), 285–294.
- Syahputra, I. (2015). Kajian hidrologi dan analisa kapasitas tampang Sungai Krueng Langsa berbasis HEC-HMS dan HEC-RAS. *Jurnal Teknik Sipil Unaya*, 1(1), 15–28.
- Waskitho, N. T. (2024). *Pengelolaan Daerah Aliran Sungai di Indonesia*. UMMPress.
- Brunner, G. W. (2022). HEC-RAS River Analysis System hydraulic reference manual (Version 6.3). U.S. Army Corps of Engineers. <https://www.hec.usace.army.mil/>
- Gunawan, G., Peri, B., Misliniyati, R., Saputra, I. K. T., Patrianusa, I., & Aqilah, H. (2023). Pemodelan genangan banjir Sub DAS Bengkulu Hilir Provinsi Bengkulu menggunakan program HEC-RAS 5.0.7 berbasis RAS Mapper dan ArcGIS 10.8. *Media Komunikasi Teknik Sipil*, 29(1), 84–92. <https://doi.org/10.14710/mkts.v29i1.53915>.
- Syarifudin, A., Satyanaga, A., & Destania, H. R. (2022). Application of the HEC-RAS program in the simulation of the streamflow hydrograph for Air Lakitan watershed. *Water*, 14(24), 4094. <https://doi.org/10.3390/w14244094>.
- Mustamin, M. R., Maricar, F., Lopa, R. T., & Karamma, R. (2024). Integration of UH SUH, HEC-RAS, and GIS in flood mitigation with flood forecasting and early warning system for Gilireng Watershed, Indonesia. *Earth*, 5(3), 274–292. <https://doi.org/10.3390/earth5030015>.
- Costache, R. (2019). Flash-flood potential assessment using GIS, remote sensing, and machine learning methods. *Science of the Total Environment*, 698, 134313. <https://doi.org/10.1016/j.scitotenv.2019.134313>
- Tehrany, M. S., Pradhan, B., & Jebur, M. N. (2014). Flood susceptibility mapping using a novel ensemble weights-of-evidence and support vector machine models in GIS. *Journal of Hydrology*, 512, 332–343. <https://doi.org/10.1016/j.jhydrol.2014.03.008>
- Merz, B., Kreibich, H., Schwarze, R., & Thieken, A. (2010). Review article: Assessment of economic flood damage. *Natural Hazards and Earth System Sciences*, 10(8), 1697–1724. <https://doi.org/10.5194/nhess-10-1697-2010>
- Bates, P. D., Horritt, M. S., & Fewtrell, T. J. (2010). A simple inertial formulation of the shallow water equations for efficient two-dimensional flood inundation modelling. *Journal of Hydrology*, 387(1–2), 33–45. <https://doi.org/10.1016/j.jhydrol.2010.03.027>

\*Correspondence author.

E-mail: [yorissaputrisupardi@gmail.com](mailto:yorissaputrisupardi@gmail.com) (Yorissa Putri Supardi)

doi: <https://doi.org/10.21771/jrtpi.2026.v17.no1.332> p100-120

2503-5010/2087-0965© 2026 Jurnal Riset Teknologi Pencegahan Pencemaran Industri-BBSPJPI (JRTPPI-BBSPJPI).

This is an open access article under the CC BY-NC-SA license (<https://creativecommons.org/licenses/by-nc-sa/4.0/>).

Accreditation number: (Ristekdikti) 158/E/KPT/2021

- Schumann, G. J. P., Bates, P. D., Horritt, M. S., & Matgen, P. (2009). Progress in integration of remote sensing-derived flood extent and stage data and hydraulic models. *Reviews of Geophysics*, 47(4). <https://doi.org/10.1029/2008RG000274>
- Apel, H., Thielen, A. H., Merz, B., & Blöschl, G. (2004). Flood risk assessment and associated uncertainty. *Natural Hazards and Earth System Sciences*, 4(2), 295–308. <https://doi.org/10.5194/nhess-4-295-2004>
- Teng, J., Jakeman, A. J., Vaze, J., Croke, B. F. W., Dutta, D., & Kim, S. (2017). Flood inundation modelling: A review of methods, recent advances and uncertainty analysis. *Environmental Modelling & Software*, 90, 201–216. <https://doi.org/10.1016/j.envsoft.2017.01.006>
- Neal, J., Schumann, G., & Bates, P. (2012). A subgrid channel model for simulating river hydraulics and floodplain inundation over large and data sparse areas. *Water Resources Research*, 48(11). <https://doi.org/10.1029/2012WR012514>
- Di Baldassarre, G., Schumann, G., Brandimarte, L., & Bates, P. D. (2011). Timely low-resolution SAR imagery to support floodplain modelling. *Journal of Hydrology*, 404(1–2), 52–66. <https://doi.org/10.1016/j.jhydrol.2011.04.027>

\*Correspondence author.

E-mail: [yorissaputrisupardi@gmail.com](mailto:yorissaputrisupardi@gmail.com) (Yorissa Putri Supardi)

doi: <https://doi.org/10.21771/jrtppi.2026.v17.no1.332> p100-120

2503-5010/2087-0965© 2026Jurnal Riset Teknologi Pencegahan Pencemaran Industri-BBSPJPI (JRTPI-BBSPJPI).

This is an open accesarticle under the CC BY-NC-SA license (<https://creativecommons.org/licenses/by-nc-sa/4.0/>).

Accreditation number: (Ristekdikti) 158/E/KPT/2021